

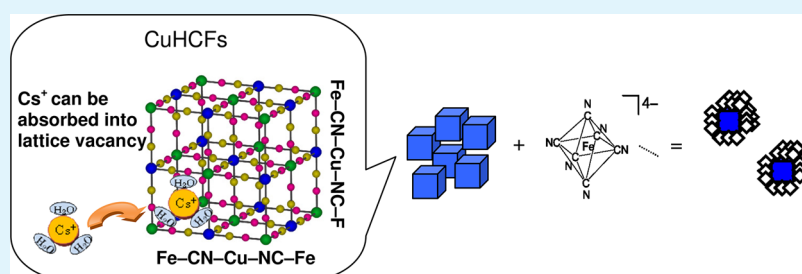
Thermodynamics and Mechanism Studies on Electrochemical Removal of Cesium Ions from Aqueous Solution Using a Nanoparticle Film of Copper Hexacyanoferrate

Rongzhi Chen,[†] Hisashi Tanaka,^{*,†} Tohru Kawamoto,[†] Miyuki Asai,[†] Chikako Fukushima,[†] Masato Kurihara,^{†,‡} Manabu Ishizaki,[‡] Masayuki Watanabe,[§] Makoto Arisaka,[§] and Takuya Nankawa[§]

[†]Nanosystem Research Institute, National Institute of Advanced Industrial Science and Technology, Tsukuba, 305-8565, Japan

[‡]Department of Material and Biological Chemistry, Faculty of Science, Yamagata University, Yamagata 990-8560, Japan

[§]Nuclear Science and Engineering Directorate, Japan Atomic Energy Agency, Tokai-mura 319-1195 Japan



ABSTRACT: Nanoparticle (NPs) film of copper hexacyanoferrate ($\text{CuHCF}^{\text{III}}$) was developed for electrochemically cesium separation from wastewater. Different from the electro- or chemical deposited films, $\text{CuHCF}^{\text{III}}$ NPs were firstly covered with ferrocyanide anions, so that they can be well dispersed in water and formed ink. Then $\text{CuHCF}^{\text{III}}$ NPs can be uniformly coated by simple wet printing methods, so it is feasible to prepare NPs film of any sizes, or any patterns at low cost. This process provided a promising technology for preparing large scale electrodes for sequential removal of Cs from wastewater in the columns. Cs separation can be controlled by an electrically switched ion exchange (ESIX) system. Effect of temperatures, and ionic strength on Cs removal was investigated. Thermodynamics results showed that Cs adsorption process was exothermic in nature and favored at low temperature. Ionic strength study indicated the $\text{CuHCF}^{\text{III}}$ film can selectively separate Cs in wide ionic strength range from 1×10^{-4} to 1×10^{-1} M Na^+ . XPS results demonstrated that the electrochemical oxidation–reduction of Fe (II/III) made contributions to Cs separation.

KEYWORDS: radiocesium, copper hexacyanoferrate, nanoparticles film, electrochemical separation, selective removal

1. INTRODUCTION

The nuclear power plant and military activities has caused a critical environmental hazard: large scale release of radiocesium,^{1,2} since ^{137}Cs is among the main fission product in radioactive wastes. In addition, accidental release of radiocesium was also reported from spent fuel reprocessing facilities.^{3,4} For instance, the megathrust earthquake and subsequent tsunami on 11 March 2011 caused annihilating damage to the Fukushima Daiichi nuclear power stations, Japan. Thousands of tons of water have been catastrophically contaminated with ^{137}Cs . Since Cs is chemically similar to sodium, the high solubility makes it easily dispersed by aqueous media and causes long term threat of radiation exposure to the biosphere.^{4,5} On the other hand, as a strong γ emitter, radiocesium can be recovered for several clinical and biotechnological applications like surgical instrument disinfection, and radiotherapy.^{6,7}

Consideration of the environmental protection and resource reuse, separation, and recovery of radiocesium from aqueous solutions is a significant and valuable issue. However, its

separation has always been one of the most challenging works in chemical engineering. From past few decades, transition metal hexacyanoferrates, in particular copper hexacyanoferrate (CuHCF), have been widely used for Cs removal from aqueous waste.^{8–13} Principally, CuHCF is chemically stable in a large pH range, and it exhibits an open zeolite type structure consisting of a cubic network of iron centers bound by bridging cyanide ligand.^{7,14} Because the cubic structure has a channel diameter of about 3.2 Å, small hydrated ion such as Cs can permeate, whereas larger hydrated ions like Na gets blocked.^{7,15} Moreover, for maintaining the charge neutrality, such structure can benefit the intercalation of alkali metal ions into the cubic network, which also contribute the selectivity of CuHCF towards cesium.

Although the structural properties of CuHCF are helpful for selective Cs separation, small-sized CuHCF particles can easily

Received: September 2, 2013

Accepted: December 2, 2013

Published: December 2, 2013

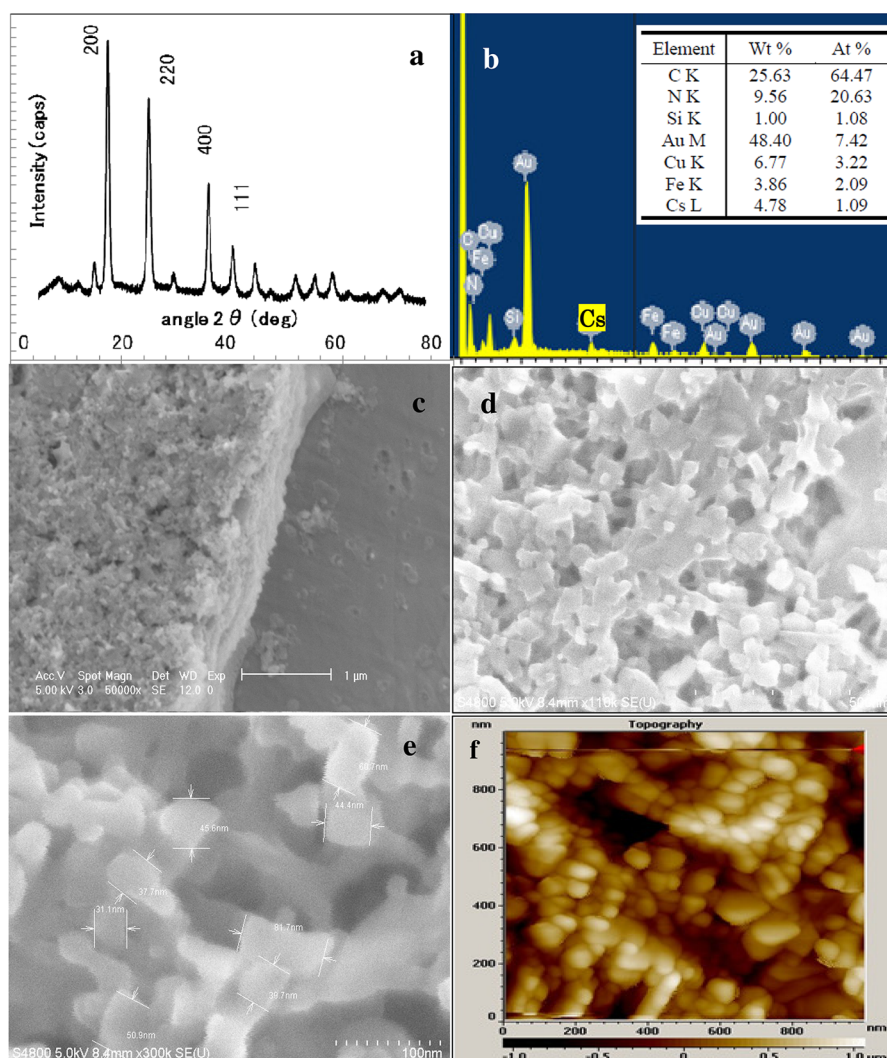


Figure 1. (a) Typical XRD pattern of Cu-HCF^{III} nanoparticle; (b) EDX result of the Cs load Cu-HCF^{III} film; FE-SEM images of nanoparticle Cu-HCF^{III} film (c) 35K \times , (d) 110K \times , (e) 300K \times , and (f) its atomic force microscopy (AFM) image.

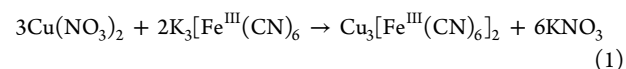
contaminate water, which restricts its direct use for column operations. To solve this problem, support materials (such as polyacrylonitrile,⁸ carboxylic latex,⁹ and mesoporous silica^{10–13}) modified CuHCF with suitable size and shape properties have been selected for Cs removal in columns. However, another key (resource reuse) for using MHCF as an adsorbent was to separate the loaded Cs from saturated adsorbents, also referred to sorbent regeneration, which is particularly challenging in utilization of these modified materials. To the best of our knowledge, it is difficult to retrieve the Cs out of the nanochannel by conventional regeneration method, once it was permeated in.

Many previous studies introduced the concept of electrochemically switched ion exchange (ESIX) as a technology using MHCF for Cs separation.¹⁶ MHCF films were electro- or chemical deposited on the electrode substance,^{17,18} Cs adsorption and desorption can be easily controlled by switching the redox states of the MHCF films to achieve ion separation and/or film regeneration.¹⁷ ESIX can separate Cs without the extra chemical reagents or filtration treatment, which lowers costs and minimizes waste generation. Besides electricity is the main driving force, fast adsorption kinetic rate can be achieved.¹⁸ However, such a technique is still difficult to

apply in wider field due to small scale of film coating (both size and thickness). To solve this issue, we first synthesized water-dispersed nanoparticle CuHCF^{III} ink and then coated its nanoparticles (NPs) on electrodes to electrochemically remove Cs. Since the CuHCF^{III} NPs can be uniformly coated by simple printing methods, it is feasible to prepare NPs film of any sizes, or any patterns at low cost. This study investigates the electrochemical Cs removal using the CuHCF NPs film and proposes a promising sorption electrode in the columns for consecutive removal and recycle of Cs from aqueous solution. Removal of Cs as a function of temperatures, and ionic strength, and the possible mechanism were also investigated.

2. EXPERIMENTAL SECTION

Preparation of CuHCF^{III} Film. The preparation of CuHCF^{III} NPs film was described in our previous study.¹⁹ In a typical run, mixture solutions of Cu(NO₃)₂·2H₂O and K₃Fe(CN)₆ were agitated in a conical tube using a vibrator (2000 rpm for 3 min). The CuHCF^{III} precipitate can be obtained, after removing the supernatant using the centrifugal separation (4000 rpm for 15 min). The chemical equation was shown as follows²⁰



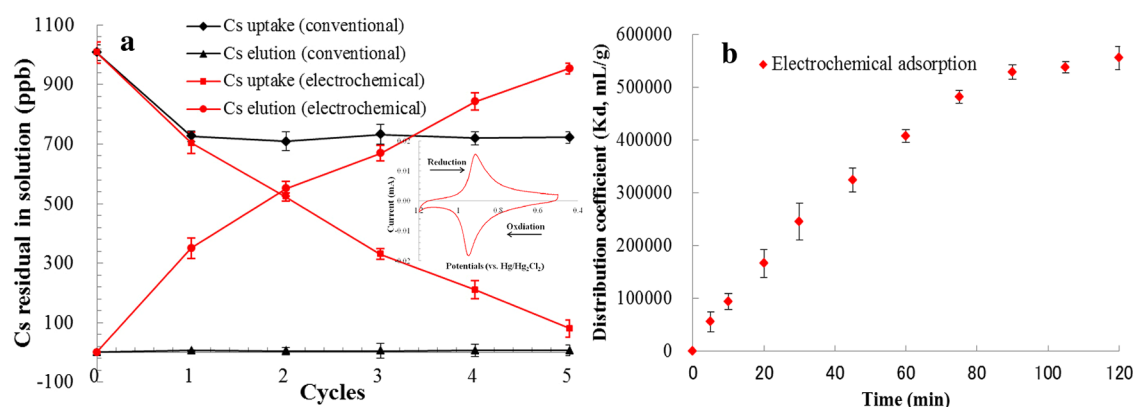


Figure 2. (a) Cesium uptake/elution using Cu-HCF^{III} film in conventional and electrochemical system (insert: cyclic voltammograms response, scan rate = 20 mV/s), and (b) effect of contact time on Cs uptake in an electrochemical system (contact time, 120 min; Cs conc., 1 ppm; pH 0.3; room temperature).

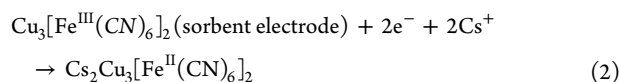
The by-product of KNO₃ was discharged by removing the supernatant. Repeat the procedure until the neutral pH of supernatant appeared. Then, the insoluble CuHCF^{III} precipitates were permeated into the solution of Na₄[Fe(CN)₆] to surface-capped [Fe^{II}(CN)₆]⁴⁻ on CuHCF^{III} NPs. So that the CuHCF^{III} was able to well disperse in water and form an ink. Finally 5% CuHCF^{III} ink was obtained for film coating on the hybrid electrodes fabricated by sputtering of 5 nm Ti and 200 nm Au (Ti/Au) on slide glass using vacuum vapor deposition (Eco engineering Ltd. Japan). Afterwards, the prepared CuHCF^{III} films were used for further characterization as well as Cs sorption.

Characterization of CuHCF^{III} Film. The CuHCF^{III} films were scanned to check the surface morphology and to estimate the particle size using a field-emission scanning electron microscope (FE-SEM, S-4800 Hitachi, Japan) and Atomic Force Microscopy (AFM). The chemical composition (atomic ratios) of the prepared samples was examined by energy-dispersive X-ray spectroscopy (EDX, EMAX300, Horiba, Japan) analysis. Structure of the CuHCF^{III} NPs was determined by an X-ray powder diffractometry (Rigaku, Japan) with CuK α beam.

X-ray photoelectron spectroscopy (XPS) experiments, performed with a Shimadzu ESCA-3400 by an Al K α X-ray source (1486.6 eV), have been used for characterizing the structure of metal compounds and the interactions with CuHCF^{III} films.²¹ A nonlinear least-square curve-fitting program (XPSPEAK software 4.1) was used to deconvolve the XPS data.²² To compensate for the charging effects, we calibrated all spectra with graphitic carbon as the reference at a binding energy (BE) of 284.8 eV.

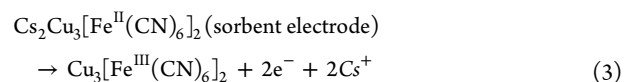
Simultaneous cyclic voltammetry (CV) and microgravimetry using an electrochemical quartz crystal microbalance (EQCM, PAR model 263A, USA) continuously detect the surface mass change on an electrode, which is useful for measuring the mass of coated CuHCF^{III} film and recording the redox response between the film and the solution.²³ The quartz crystal was a 9 MHz AT-cut quartz crystal with gold electrodes (diameter: 5 mm).

Electrochemical Separation (ES) of Cesium. A three-electrode cell, in which an SCE (Hg/Hg₂Cl₂/KCl saturated solution) as the reference electrode, a platinum electrode as the counter electrode, and the CuHCF^{III} film coated electrode as the working electrode (2.5 × 2.0 cm²), was used for electrochemical separation of Cs.²⁴ For Cs uptake from wastewater, the CuHCF^{III} film coated electrodes were impregnated to electrolyte solutions containing CsNO₃ and 1 ppm NaNO₃. The redox reaction for uptake process by Multi-potential step (MPS) technique from +1.3 V to 0 V (vs. SCE) was described as follows



The reactions were performed at a constant speed of 450 rpm using a magnetic stirring, and room temperature (22 °C).

For Cs elution, the Cs loaded electrodes were transferred into a Milli-Q solution containing 1 ppm NaNO₃, which was used for enhancing the conductivity of the elution. The elution was also operated using MPS technique by switching the applied potentials of the CuHCF^{III} film, from 0 V to +1.3 V. The redox reaction for Cs elution process was proposed as follows



Each Cs uptake and elution was performed for 30 min respectively, and samples were taken at certain intervals to measure Cs concentration by inductively coupled plasma mass spectrometer (ICP-MS, NexIon300 D, PerkinElmer, USA).

The distribution coefficient (K_d), measured as a function of contact time, was used to estimate the selectivity for Cs.

$$K_d (\text{mL/g}) = (C_0 - C_t) / CtV/M \quad (4)$$

where C_0 and C_t stand for the Cs concentration at initial stages and time t , respectively, V is the solution volume and M is the mass of sorbents. The effects of some parameters such as, reaction temperatures (from 298, to 323 K), and ionic strength (from 1×10^3 to 1×10^5 ppm of NaNO₃ solution) were studied.

3. RESULTS AND DISCUSSION

CuHCF^{III} Nanoparticle and Sorbent Electrodes. The crystal structure of the CuHCF^{III} nanoparticle was analyzed by X-ray diffraction (XRD) pattern in Figure 1a. The peaks at 17.64, 25.04, and 35.71° are attributed to the Miller indexes of (2 0 0), (2 2 0), and (4 0 0) of the diffraction planes, respectively, indicating the cubic crystalline structure of Cu[Fe(CN)₆]_{0.667}. The average crystallite size of the CuHCF^{III} NPs was evaluated as 20 nm according to Scherrer's formula ($D = K\lambda/\beta\cos\theta$), in which the full width at half maximum β of the diffraction peak with the Bragg angle of θ .²⁵ SEM-EDX technique was used for examining the elements distribution and chemical compositions of the CuHCF^{III} film. As shown in Figure 1b, after 1 ppm Cs sorption the EDX results indicated that the existence of elements of Fe, Cu, C, and N, which can be coded as CuHCF^{III}. Furthermore, the atom ratio of Cu/Fe was 3.22:2.09, closed to the prepared CuHCF^{III} core (3:2).²⁴ Cs signals were also detected, referring to the Cs loading after adsorption. The XRD and EDX results confirmed the successful synthesis of CuHCF^{III} NPs film.

The FE-SEM images of the CuHCF^{III} film (Figure 1c–e) demonstrate that a film abundant in slits was formed on the surface of the electrodes, which might facilitate the mass

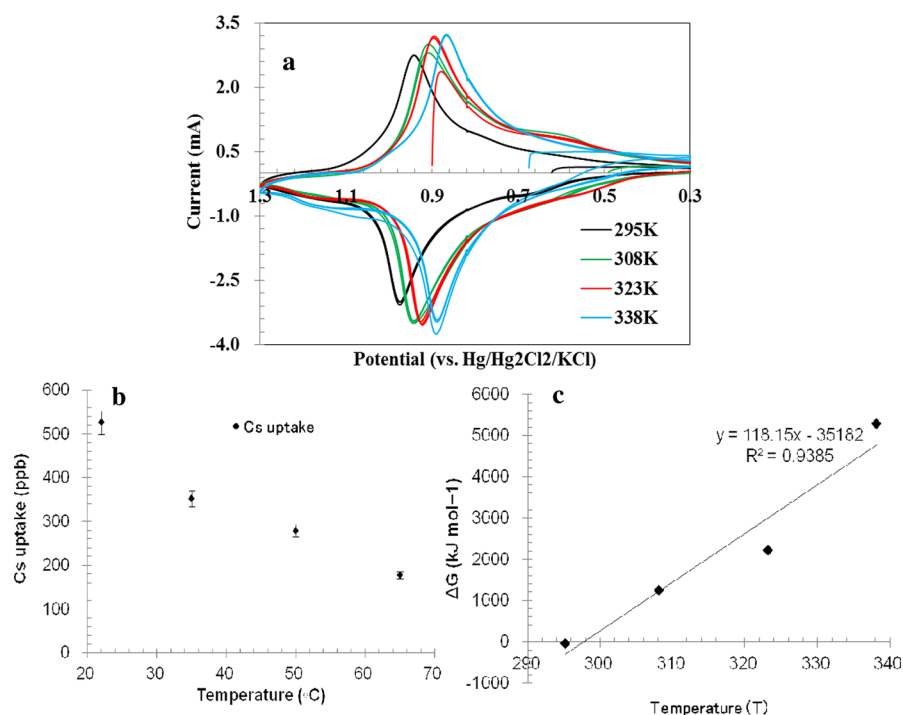


Figure 3. (a) Microgravimetric cyclic voltammograms (CV) of a $\text{CuHCF}^{\text{III}}$ film employed in 0.1 M CsNO_3 electrolyte under different temperatures (from 298 to 338 K), (b) effect of temperature on Cs sorption using $\text{Cu-HCF}^{\text{III}}$ films, and (c) their corresponding thermodynamic parameters.

transfer and diffusion of Cs in adsorption.²² The clear geometric particles with a single particle dimension of approximately 20 nm was coincident with the XRD results. The harsh surface of the electrode with well dispersed heterogeneous nanoparticles was observed by AFM in Figure 1f. This will lead to an increase in its specific area throughout the binding matrix, which will benefit for Cs removal. Because of the estimation from the agglomeration of particles, AFM indicated the size of particles ranged from 20 to 80 nm, which was different from SEM and XRD results.

The mass of $\text{CuHCF}^{\text{III}}$ film was measured by EQCM equipment. According to the Sauerbrey equation,²⁶ the mass change on the quartz surface (Δmass) is proportional to the induced change of the resonance frequency Δfreq ²⁴

$$\Delta\text{mass} = \frac{-\Delta\text{freq}A\sqrt{\mu_q\rho_q}}{2F_qF} \quad (5)$$

μ_q is the consistency of AT cut quartz crystal, 2.947×10^{11} g/cm²s²; ρ_q is the density of AT cut quartz crystal, 2.648 g/cm³; F_q is the standard frequency 9.0 MHz; A is the working area of AT cut quartz crystal, 0.196 cm². Through the calculation, the mass of coated $\text{CuHCF}^{\text{III}}$ film on the Ti/Au electrode was approximately 192.1 μg .

Electrochemical Separation. Electrochemical separation using the prepared $\text{CuHCF}^{\text{III}}$ film was performed in 1 ppm $\text{CsNO}_3/\text{NaNO}_3$ electrolyte for Cs uptake, and then translated into 1 ppm NaNO_3 electrolyte for Cs elution, respectively. Repeated the procedure 5 cycles, and the Cs concentrations measured by ICP-MS were shown in Fig. 2. About 92.05% of total Cs was adsorbed on the $\text{CuHCF}^{\text{III}}$ film, because of the electrochemical reduction from Cu(II)-CN-Fe(III) to Cu(II)-CN-Fe(II) . Contrarily, more than 97.22% of the adsorbed Cs was desorbed from the loaded $\text{CuHCF}^{\text{III}}$ film. The results indicated that the Cs loaded film can be successfully

regenerated by a reversible oxidation from Cu(II)-CN-Fe(II) to Cu(II)-CN-Fe(III) . Cs uptake and elution can be simply regulated by switching the applied potentials of the $\text{CuHCF}^{\text{III}}$ film.

In the primary stage, experiments using electrodes without the $\text{CuHCF}^{\text{III}}$ film indicated no Cs redox response or Cs uptakes. For comparison, we also did the conventional adsorption/desorption experiments, in which the similar $\text{CuHCF}^{\text{III}}$ film were impregnated in Cs solution without any electrochemical operation, and other experimental conditions (such as, pH, temperature, and initial Cs concentrations) were extremely same as the electrochemical separation. The removal efficiency was quite similar as that in ES at the 1st cycle (Figure 2a). However, Cs concentration almost showed no changes from the 2nd cycle, which was because the Cs adsorption process reached its saturation equilibrium after 1st cycle adsorption. Namely, the NPs film could not be reused or regenerated under the conventional condition. It also confirmed that Cs separation was mainly caused by the electrochemical redox between the Cu(II)-CN-Fe(II) and Cu(II)-CN-Fe(III) . Comparing with the conventional method, the effective regeneration performance in ES suggested a promising sorbent for recycle utilization. In order to investigate the effect of reaction time, Cs removal using the $\text{CuHCF}^{\text{III}}$ film has been continuously performed for 2 h. As shown in Figure 2b, the Cs adsorption increased with reaction time increase, until the saturation equilibrium state reached after 120 min, while the distribution coefficient (K_d) for Cs was in excess of 5.6×10^5 mL/g.

The pH effect on Cs removal was studied by a series of experiments in various solutions of initial pH from 0.2 to 11.0.¹⁹ Cs removal showed stable performance from pH 0.2 to 8.9, following a sudden decrease when pH was over 11.0. This was because the negatively charged Cs hydroxides began to

form at pH greater than 11.0, which caused a decrease in Cs uptake due to the electrostatic repulsion.

Effect of Temperature. The temperature is an important parameter to affect the transport/kinetic process of reactions, especially to electrochemical reactions. To examine the effect of temperature, we conducted electrochemical characterization of CuHCF^{III} film and its Cs uptakes at 298, 313, and 323 K, respectively. CV results demonstrated the formal potentials E_f of the redox system $[\text{Fe}(\text{CN})_6]^{3-/4-}$, calculated as a half of the sum of potentials of anodic and cathodic current peaks,²⁷ was proved to be strongly dependent on the temperature.²⁸ It was observed that E_f shifts to the negative direction, namely the potential becomes more cathodic, when the temperature raised (Figure 3a). This meant that the equilibrium of the redox process $[\text{Fe}(\text{CN})_6]^{3-} + e^- \rightarrow [\text{Fe}(\text{CN})_6]^{4-}$ shifts to the left direction with an increase of the temperature, in other words, the findings revealed that upon decreasing temperature the Cs loading (reduction of $[\text{Fe}(\text{CN})_6]^{4-}$ to $[\text{Fe}(\text{CN})_6]^{3-}$) is a more favorable process than the Cs unloading (oxidation of $[\text{Fe}(\text{CN})_6]^{3-}$ to $[\text{Fe}(\text{CN})_6]^{4-}$).²⁹ This finding was in absolute agreement with the Cs uptake results, in which Cs removal decreased with the increase in temperature (Figure 3b). Namely, the Cs redox process was exothermic in nature.

To study the feasibility of the sorption process, the thermodynamic parameters such as, changes in the Gibbs free energy (ΔG), enthalpy (ΔH), and entropy (ΔS) can be calculated by the following equations³⁰

$$\log K_c = C_{Ac}/C_e \quad (6)$$

$$\Delta G = -RT \ln K_c \quad (7)$$

$$\Delta G = \Delta H - T\Delta S \quad (8)$$

where R is the universal gas constant (8.314 J/(mol K)) and T is absolute temperature in Kelvin. K_c is the ratio of Cs adsorbed on CuHCF^{III} film (q_e) to the residual Cs in solution (C_e) at equilibrium state, ΔH and ΔS are calculated from the slope and intercept of the linear plot of $\ln K_c$ versus $1/T$.

As presented in Fig. 3c, when the temperature increased from 295 to 338 K, ΔG was increased from -0.153 to 3.453 kJ/mol. This indicated that the adsorption was favored at lower temperatures. The negative values of ΔG at 298 K indicated the Cs adsorption process on CuHCF^{III} films was an exergonic or spontaneous process. With the temperature increase, the positive ΔG indicated the unfavorable reaction tendency. Nevertheless, the negative value of ΔH confirmed the adsorption process is an exothermic nature. Tsierkezos et al.²⁸ reported similar results, in which the reduction process of $[\text{Fe}(\text{CN})_6]^{3-}$ to $[\text{Fe}(\text{CN})_6]^{4-}$ was exothermic and released energy. However, an endothermic reaction for Cs adsorption on copper hexacyanoferrate–polyacrylonitrile composite has been reported by Nilchi et al.,³¹ who indicated that the ion exchanger takes the main effect on the Cs sorption reaction.

Effect of Ionic Strength. The effect of ionic strength was studied by adding varying concentrations of Na^+ into Cs^+ solutions. The results revealed that the K_d values showed insignificant change, when Na^+ concentration increased from 1×10^{-4} to 1×10^{-1} M, indicating Na^+ has negligible influence on Cs^+ removal. Figure 4a shows that the CV responses of our CuHCF^{III} film employed in these mixture solutions. For comparison, measurement in pure CsNO_3 and NaNO_3 solution were also performed.

As shown in Fig. 4a, in the pure NaNO_3 solution, a couple of cathodic and anodic peak current were observed at the 0.5 V

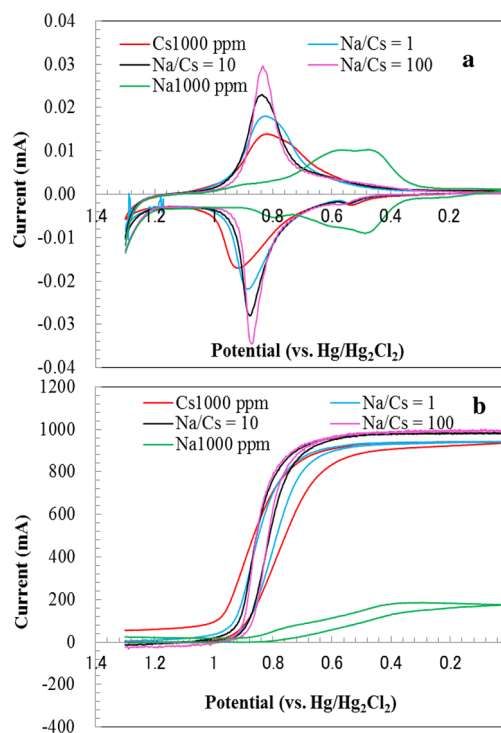


Figure 4. (a) CV of a CuHCF^{III} film employed in 1000 ppm pure NaNO_3 , CsNO_3 electrolyte, and in the mixture solution with Na/Cs proportion from 1 to 100, (b) the mass change in EQCM recorded concurrently with the CV of a, scan rate = 5 mV/s.

(vs. $\text{Hg}/\text{Hg}_2\text{Cl}_2$), relating to the redox process of $\text{Cu}_3[\text{Fe}^{\text{III}}(\text{CN})_6]_2/\text{Na}_2\text{Cu}_3[\text{Fe}^{\text{II}}(\text{CN})_6]_2$.³² However, once the Cs ion were added in, no matter how large the Na/Cs is, only one redox couple appeared on CV response. Furthermore, its CV peak was close to the solution containing pure CsNO_3 , thus the redox peaks corresponded to the $\text{Cu}_3[\text{Fe}^{\text{III}}(\text{CN})_6]_2/\text{Cs}_2\text{Cu}_3[\text{Fe}^{\text{II}}(\text{CN})_6]_2$ redox couple. Mass change in EQCM record (Fig. 4b) demonstrated that mass on CuHCF^{III} film, corresponded to the loaded Cs, slightly increased with the increasing of Na/Cs . This finding indicated Na not only has no competing effect to Cs adsorption, but also gave an elevating effect to Cs uptake, due to the enhancement of the ionic strength. This can also be noticed by the peak increasing trend of CV response in the mixture solutions. No Na^+ response was found in the presence of Cs^+ , indicating the CuHCF^{III} films have a prior selectivity for cesium.

We also investigated the effect of Cs removal when some chemically similar ions (Li^+ , Na^+ , K^+ and Rb^+) coexisted in the solutions. Results indicated Cs removal decreased in the series: $\text{Li}^+ < \text{Na}^+ < \text{K}^+ < \text{Rb}^+$,¹⁹ due to the size dependency of cation insertion into the CuHCF lattice.³¹ However, comparing with results from pure CsNO_3 solution, the insignificant influence indicated that CuHCF^{III} film can selectively separate Cs.

Possible Mechanism. Cs separation using the CuHCF^{III} films was achieved during the hexacyanoferrate (II/III) reaction. Thus, the iron valence (oxidation state) has been recognized as a key role in determining the mechanism of Cs sorption. In order to investigate film–cesium interactions, X-ray photoelectron spectroscopy (XPS) was utilized to identify the sorption sites involved in the accumulation of Cs species and to determine the changes of the iron valence.²¹

Fig. 5a depicts the typical XPS spectra for CuHCF^{III} films before adsorption, and after 3 min, 90 min adsorption (coded as

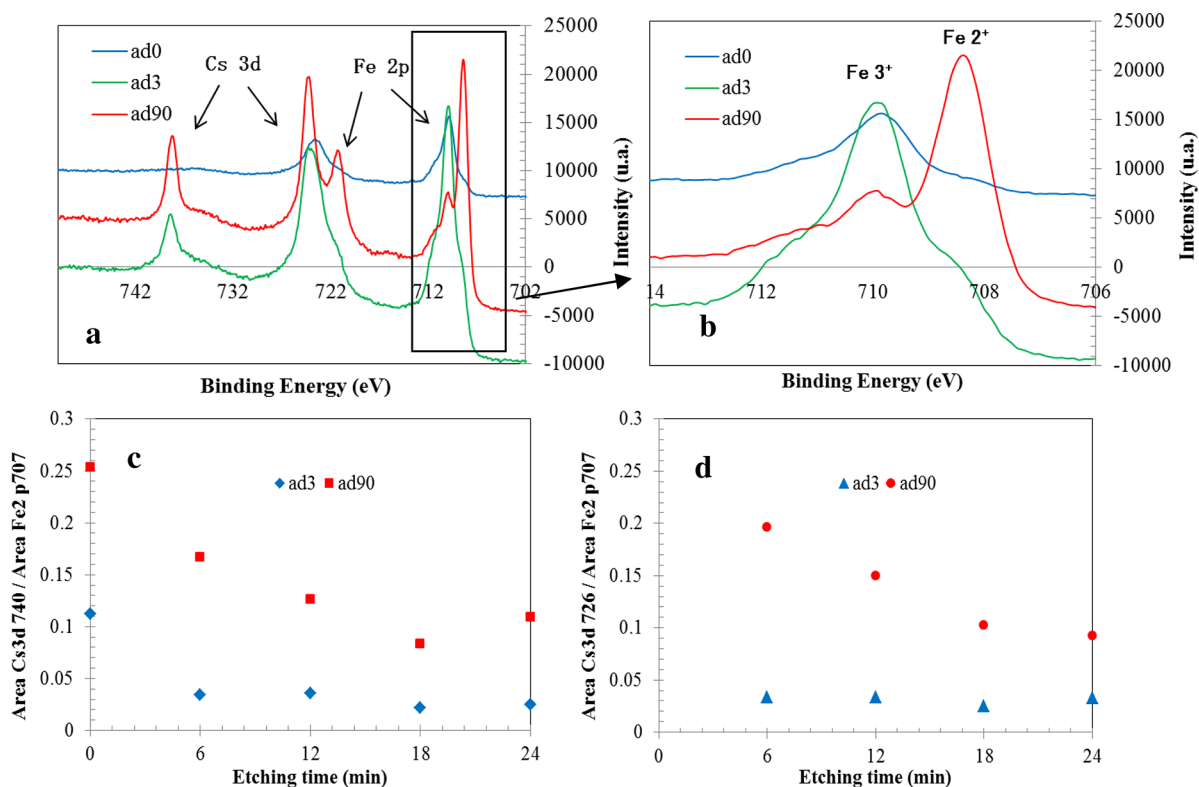


Figure 5. (a) XPS survey scan of Cs 3d, Fe 2p and (b) high-resolution spectra of Fe 2p for Cu-HCF^{III} films before sorption and after 3 and 90 min sorption (coded as ad0, ad3, and ad90, respectively), and etching results: (c) proportion of peak area $Cs_{3d\ 740} / area_{Fe2p\ 707}$, (d) proportion of peak area $Cs_{3d\ 726} / area_{Fe2p\ 707}$.

ad0, ad3 and ad90, respectively). Comparing with unused film, the appearance of peaks for Cs 3d at 724 and 738 eV indicated the Cs ions were adsorbed on film surface. Obviously, the peak of ad90 is much higher than that of ad3. The binding energy for Fe 2p are assigned at 707 eV to Fe(II), whilst Fe(III) are characterized at higher binding energies such as 710 eV. Fig. 5b indicated both Fe(II) and Fe(III) were observed in spectra of ad90. There are two explanations, one is that electrochemical reduction of Cu(II)-CN-Fe(III) to Cu(II)-CN-Fe(II) partly occurred on the surface of the film.²³ Another one is that all Fe(III) was firstly reduced to Fe(II), subsequently part of Fe(II) was oxidized to Fe(III) again in the open air. However, in ad3 spectra only Fe(III) specie appeared, which is similar as the result from the unused film. We assumed that 3 min might be too short for the electrochemical redox reaction, and thus no Fe(II) was observed.

To explore the iron oxidation state underneath the surface layer, we bombarded the CuHCF^{III} films by 5 keV argon ion using etching technology, the depth profile spectrum was shown in Figure 6. The BEs assigned at 720 eV, confirming the reduction of Fe(III). However, we also find the same iron oxidation state in ad3. This may be because of the photo-reduction by Argon ion etching. We calculated the peak area proportion of Cs3d/Fe2p707, and translate the data into Figure 5c, d. It is clear that the proportion in ad90 decreased with etching time increased, which means the Cs sorption was not only occurred on the surface layer, but also slowly permeated into the mesosphere. While the proportion in ad3 showed no difference, indicating sorption mainly occurred on the surface layer. Because no redox reaction occurred, such a surface reaction might be due to conventional sorption.

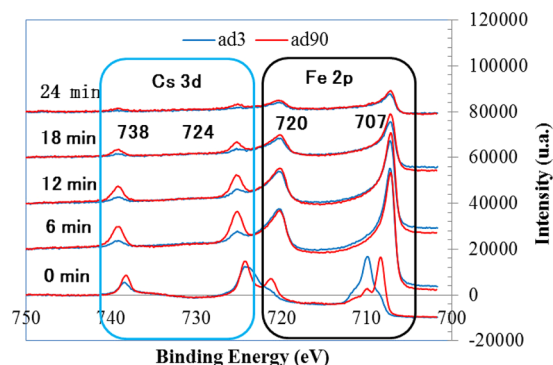


Figure 6. Depth profile XPS spectrum of the Cu-HCF^{III} films bombarded by 5 keV Argon ion using etching technology (etching time 24 min).

4. CONCLUSION

The synthesized CuHCF^{III} film, which has a crystalline structure, nanoparticle morphology, and high selectivity for cesium, was proposed for Cs separation in an ESIX system. Cs separation can be easily controlled by electrochemical oxidation–reduction of CuHCF^{III} film, without any costly ion-exchange membrane or extra chemical reagents. Thermodynamic study indicated Cs uptake was exothermic in nature. Effective Cs separation can be adopted at a wide range of pH (0.2 to 8.9) and ionic strength (1×10^{-4} to 1×10^{-1} M Na⁺). Minimization of secondary waste, simple regeneration and easy operation suggest a promising technology for removal of Cs. Because of the high cost of Au hybrid electrodes, the inexpensive stainless sheets will be taken as alternative electrode for large surface film coating. In the future, the

rolled sheet electrodes will be used in columns for sequential removal of Cs from actual wastewater, and the durability of the column system will also been investigated.

AUTHOR INFORMATION

Corresponding Author

*E-mail: hisashi.tanaka@aist.go.jp. Tel: +81-29-861-5141.

Notes

The authors declare no competing financial interest.

ACKNOWLEDGMENTS

A part of this study is the result of "Compact and reusable cesium recovery system by electrochemical adsorption/desorption" carried out under the Strategic Promotion Program for Basic Nuclear Research by the Ministry of Education, Culture, Sports, Science and Technology of Japan (MEXT).

REFERENCES

- (1) Lykknes, A. *Endeavour* **2005**, *29*, 136.
- (2) Ararem, A.; Bouras, O.; Arbaoui, F. *Chem. Eng. J.* **2011**, *172*, 230–236.
- (3) Zachara, J.M.; Smith, S.C.; Liu, C.X.; Mckinley, J.P.; Serne, R.J.; Gassman, P.L. *Geochim. Cosmochim. Acta.* **2002**, *66*, 193–211.
- (4) Wang, T.H.; Li, M.H.; Wei, Y.Y.; Teng, S.P. *Appl. Radiat. Isot.* **2010**, *68*, 2140–2146.
- (5) Andersson, K.G.; Roed, J.; Fogh, C.L. *J. Environ. Radioact.* **2002**, *62*, 49–60.
- (6) Ebner, A.D.; Ritter, J.A.; Navratil, J.D. *Ind. Eng. Chem. Res.* **2001**, *40*, 1615–1623.
- (7) Parab, H.; Sudersanan, M. *Water Res.* **2010**, *44*, 854–860.
- (8) Nilchi, A.; Saberi, R.; Moradi, M.; Azizpour, H.; Zarghami, R. *Chem. Eng. J.* **2011**, *172*, 572–580.
- (9) Avramenko, V.; Bratskaya, S.; Zheleznov, V.; Sheveleva, I.; Voitenko, O.; Sergienko, V. *J. Hazard. Mater.* **2011**, *186*, 1343–1350.
- (10) Sangvanich, T.; Sukwarotwat, V.; Wiacek, R.J.; Grudzien, R.M.; Fryxell, G.E.; Addleman, R.S.; Timchalk, C.; Yantasee, W. *J. Hazard. Mater.* **2010**, *182*, 225–231.
- (11) Lin, Y.; Fryxell, G.E.; Wu, H.; Engelhard, M. *Environ. Sci. Technol.* **2001**, *35*, 3962–3966.
- (12) Loos-Neskovic, C.; Ayrault, S.; Badillo, V.; Jimenez, B.; Garnier, E.; Fedoroff, M.; Jones, D.J.; Merinov, B. *J. Solid State Chem.* **2004**, *177*, 1817–1882.
- (13) Han, F.; Zhang, G.H.; Gu, P. *J. Hazard. Mater.* **2012**, *225*, 107–113.
- (14) Keggin, J.F.; Miles, F.D. *Nature* **1936**, *137*, 577–578.
- (15) Pyrasch, M.; Toutianoush, A.; Jin, W.Q.; Schnepf, J.; Tieke, B. *Chem. Mater.* **2003**, *15*, 245–254.
- (16) Lilga, M.A.; Orth, R.J.; Sukamto, J.P.H.; Rassat, S.D.; Genders, J.D.; Gopal, R. *Sep. Purif. Technol.* **2001**, *24*, 451–466.
- (17) Hao, X.G.; Li, Y.G.; Pritzker, M. *Sep. Purif. Technol.* **2008**, *63*, 407–414.
- (18) Sun, B.; Hao, X.G.; Wang, Z.D.; Guan, G.Q.; Zhang, Z.L.; Li, Y.B.; Liu, S.B. *J. Hazard. Mater.* **2012**, *233–234*, 177–183.
- (19) Chen, R.; Tanaka, H.; Kawamoto, T.; Asai, M.; Fukushima, C.; Kurihara, M.; Watanabe, M.; Arisaka, M.; Nankawa, T. *Electrochem. Commun.* **2012**, *25*, 23–25.
- (20) Gotoh, A.; Uchida, H.; Ishizaki, M.; Satoh, T.; Kaga, S.; Okamoto, S.; Ohta, M.; Kawamoto, T.; Tanaka, H.; Kurihara, M.; et al. *Nanotechnology* **2007**, *18*, 345609.
- (21) Vieira, R.S.; Oliveira, M.L.M.; Guibal, E.; Castellon, E.R.; Beppu, M.M. *Colloids Surf, A* **2011**, *374*, 108–114.
- (22) Zhang, S.J.; Li, X.Y.; Chen, J.P. *J. Colloid Interface Sci.* **2010**, *343*, 232–238.
- (23) Chen, S.M.; Chan, C.M. *J. Electroanal. Chem.* **2003**, *543*, 161–173.
- (24) Chen, R.; Tanaka, H.; Kawamoto, T.; Asai, M.; Fukushima, C.; Na, H.; Kurihara, M.; Watanabe, M.; Arisaka, M.; Nankawa, T. *Electrochim. Acta.* **2013**, *87*, 119–125.
- (25) Chan, K.Y.; Teo, B.S. *Microelectron. J.* **2007**, *38*, 60–62.
- (26) Reddy, S.J.; Dostal, A.; Scholz, F. *J. Electroanal. Chem.* **1996**, *403*, 209–212.
- (27) Batterjee, S.M.; Marzouk, M.I.; Aazab, M.E.; El-Hashash, M.A. *Appl. Organomet. Chem.* **2003**, *17*, 291–297.
- (28) Tsierkezos, N.G.; Ritter, U. *J. Chem. Thermodyn.* **2012**, *54*, 35–40.
- (29) Yamashita, H.; Yamaguchi, S.; Nishimura, R.; Maekawa, T. *Anal. Sci.* **2001**, *17*, 45–50.
- (30) Karamanis, D.; Assimakopoulos, P.A. *Water Res.* **2007**, *41*, 1897–1906.
- (31) Nilchi, A.; Saberi, R.; Moradi, M.; Azizpour, H.; Zarghami, R. *Chem. Eng. J.* **2011**, *172*, 572–580.
- (32) Chang, C.Y.; Chau, L.K.; Hu, W.P.; Wang, C.Y.; Liao, J.H. *Microporous Mesoporous Mater.* **2008**, *109*, 505–512.